Supplementary Materials

GNNSynergy: A Multi-view Graph Neural Network for Predicting Anti-cancer Drug Synergy

Zhifeng Hao, Jianming Zhan, Yuan Fang, Min Wu and Ruichu Cai*

December 19, 2021

Abstract

This report gives supplementary information to the manuscript "GNNSynergy: A Multi-view Graph Neural Network for Predicting Anti-cancer Drug Synergy". It provides more detailed information about dataset, parameter setting for baseline methods and GNNSynergy, as well as some additional experimental results.

1 Experimental Data

Table S1 shows the cancer cell lines included in the DrugComb database. There are 81 cell lines originated from 11 different tissues.
We performed the t-SNE analysis to visualize the cell lines in 2D space to reflect relationships among them in Fig. S1. Originally, each cell line has 972 features for its gene expression profile, and here we applied t-SNE to map the 972-dimensional vectors into the 2D space. It shows that cell lines within the same tissues are closer to each other. Given a specific cell line, the information of other cell lines in the same tissue would be useful for drug synergy prediction.

2 Parameter Setting and Sensitivity Analysis

2.1 Hyper-parameter Setting

The hyper-parameters of all the methods were optimized by the validation set, using grid search. Table S2 shows the search range for different hyper-parameters in the baseline methods, including Elastic Net (EN), Random Forest (RF), Gradient Boosting Machine (GBM), TreeCombo (XGBoost) and comboLTR. For the deep learning methods, such as DeepSynergy, TranSynergy and MatchMaker, we used the default parameters used in their original papers.

Table S1: **The 81 cell lines tested in the DrugComb Database, covering 11 different tissue types. Amount indicated the amount of cell lines in the tissue.**

Tissue (# cell lines)	Number of drug pairs	Cell Line
Large Intestine (10)	35297	SW-620; HT29; HCT116; HCT-15; KM12; COLO 205; HCC-2998; LOVO; SW837; RKO
Breast (8)	29421	T-47D; MDA-MB-231; MCF7; BT-549; MDA-MB-468; HS 578T; OCUBM; MDAMB436;
Lymphoid (8)	25234	K-562; CCRF-CEM; SR; MOLT-4; RPMI-8226; L-1236; HDLM-2; L-428;
Kidney (8)	37363	ACHN; SN12C; TK-10; A498; 786-0; CAKI-1; UO-31; RXF 393;
Lung (13)	39934	NCIH23; NCI-H226; A549; EKVX; NCI-H322M;NCI-H522; HOP-92; HOP-62; A427; SKMES1;NCIH2122; NCIH520; NCIH1650
Ovary (11)	31186	SK-OV-3; OVCAR3; OVCAR-5; IGROV1; OVCAR-8; OVCAR-4; A2780; PA1; ES2; UWB1289; OV90;
Skin (11)	33389	UACC62; UACC-257; SK-MEL-28; SK-MEL-5; M14;LOX IMVI; SK-MEL-2; A375; RPMI7951; A2058; HT144
Brain (6)	24883	SF-268; U251; SF-539; SF-295; SNB-75; T98G
Prostate (3)	9872	PC-3; DU-145; VCAP
Bone (2)	1878	A-673; TC-71
Soft (1)	80	RD

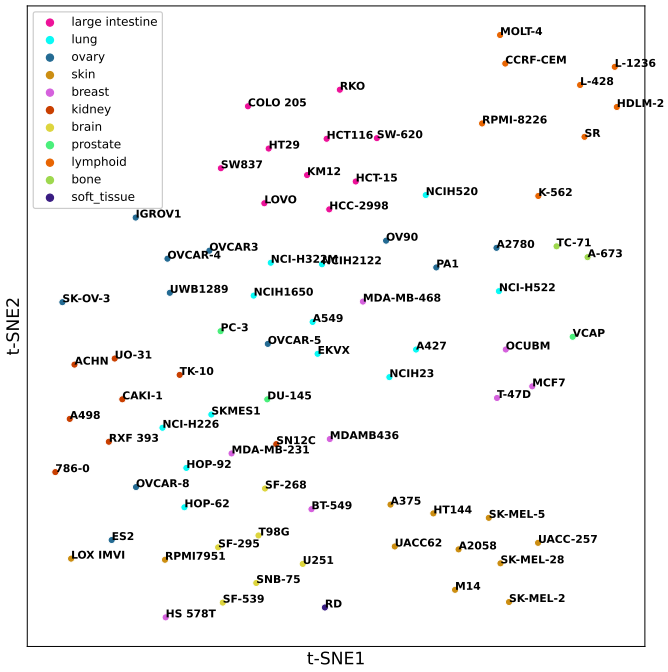

Figure S1: Visualization of different cell lines with t-SNE analysis. Different colors indicate different tissues. It shows that cell lines within the same tissues are closer to each other.

Table S2: **Hyper-parameters for Baselines**

Model	Hyperparament	Values consided
EN	Constant α	0.001; 0.01; 0.1; 1; 10; 100
	L1 ratio	0.2; 0.4; 0.6; 0.8
RF	numbers of estimators (decision trees)	10; 100; 500; 1000
	maximum tree depth	4; 6; 8; 10; 12
GBM	numbers of estimators (decision trees)	10; 100; 500; 1000
	maximum tree depth	4; 6; 8; 10; 12
	learning rate	0.05; 0.10; 0.15
XGBoost	maximum tree depth	4; 6; 8; 10; 12
	learning rate	0.05; 0.10; 0.15
comboLTR	rank_uv	20; 32; 64; 128; 256
	repeats	20; 70; 120; 170; 220; 270
	ranks	20; 40; 60; 80; 100

For our GNNSynergy, we used 1-layer GCN with output feature dimensionality $d = 256$ and dropout rate $\rho = 0.7$. We used 4-layer MLPs (i.e., 1 input layer, 2 hidden layers and 1 output layer) in both single-view and multi-view encoders. The input layer of MLPs in single-view encoder has $3d = 768$ neurons, and it has $3d \times k$ neurons in multi-view encoder with k sub-view cell lines. For MLPs in single-view encoder, their 2 hidden layers and 1 output layer had 256, 512 and 256 neurons, respectively, and the dropout rates for 2 hidden layers were set as 0.5 and 0.2. For MLPs in multi-view encoder, their 2 hidden layers and 1 output layer had 1280, 512 and 256 neurons, respectively, and the dropout rates for 2 hidden layers were set as 0.5 and 0. Note that we pre-trained the single-view encoder for each cell line with a learning rate of 1e-3, while the learning rate to optimize the overall GNNSynergy model was set as 1e-5. Lastly, we set the maximum number of training epochs to 2000, and we considered the early-stop mechanism that the optimization will stop if the validation loss does not decline within the recent 300 epochs. Table S3 summarizes the parameter settings in our GNNSynergy.

Table S3: **Hyper-parameter settings for GNNSynergy**

Module	Hyperparameter	Value
Global	learning rate in single-view (η_1)	1e-3
	learning rate in multi-view (η_2)	1e-5
	max epoch	2000
	early-stop epoch	300
GCN	dimensionality (d)	256
	dropout probability (ρ)	0.7
MLP in Single-View	dimensionality	[256, 512, 256]
	dropout probability (β)	[0.2,0.5]
MLP in Multi-View	dimensionality	[1280, 512, 256]
	dropout probability (γ)	[0.0, 0.5]

2.2 Parameter Sensitivity Analysis

We present the sensitivity analysis for the parameters in our GNNSynergy, including the GCN dimensionality d, GCN dropout probability ρ, the dropout probability β_1, β_2 of MLP in Single-View, and the dropout probability γ_1, γ_2 of MLP in Multi-View, as shown in Fig. S2.

From the Fig. S2(a), the performance of GNNSynergy is relatively stable when ρ is set as different values. Thus, we recommend to set ρ in the range $[0.5, 0.9]$. In Fig. S2(b), we could observe that the medium values for d e.g., $d = 2^7$ or $d = 2^8$ are more favorable. In our study, we used $d = 2^8 = 256$. Fig. S2(c) and Fig. S2(d) show the performance of GNNSynergy using different values for β_1 and β_2 (the dropout probabilities in MLPs in single-view encoder), respectively. We change one of them and fix the other to its default value. As for β_1, we can observe that the MSE of GNNSynergy starts to increase when β_1 is larger

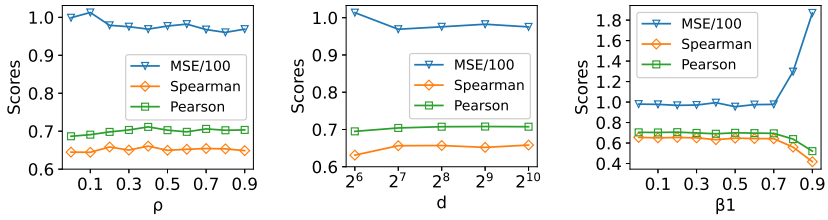

(a) GCN Dropout probability ρ (b) GCN Dimensionality d (c) Dropout probability β_1

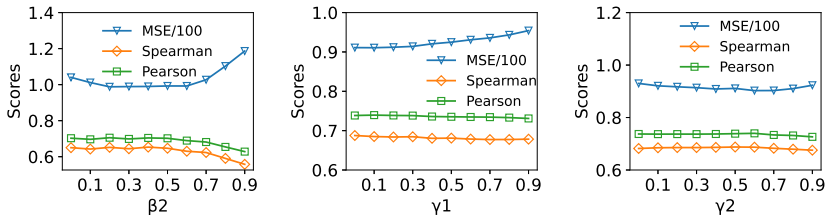

(d) Dropout probability β_2 (e) Dropout probability γ_1 (f) Dropout probability γ_2

Figure S2: Parameter sensitivity analysis for GNNSynergy.

than 0.7. Similarly, the performance get worse when $\beta_2 > 0.5$. In this paper, we set β_1 as 0.2 and β_2 as 0.5 in our experiments. In Fig. S2(e) and Fig. S2(f), we can observe that GNNSynergy achieves the best performances when $\gamma_1 = 0, \gamma_2 = 0.5$.

2.3 Impact of Threshold t

As mentioned in the main manuscript, we construct 3 drug-drug synergy graphs for each cancer cell line based on a pre-defined threshold $t = 10$. Although this setting is following other previous studies, we still would like to show the impact of this parameter on the model performance. We evaluate the performance of GNNSynergy when t is set as different values, e.g., 0, 10, 20 and 30. Table S4 shows that GNNSynergy achieves the best performance when $t = 10$. Note that we have two DDS graphs only when $t = 0$.

Table S4: **The performance of GNNSynergy when t is set as different values.**

Values	MSE	RMSE	MAE	Sperman	Pearson
$t = 0$	95.308	9.618	6.469	0.651	0.699
$t = 10$	88.691	9.278	6.168	0.696	0.742
$t = 20$	94.049	9.544	6.406	0.655	0.710
$t = 30$	95.185	9.596	6.459	0.656	0.711

3 Results

3.1 Performance for Individual Cell Lines

In our main manuscript, we showed the average performance of various methods over all the cell lines. Here, we further investigated the performance of GNNSynergy on each individual cell line. The spearman correlation coefficients and pearson correlation coefficients for GNNSynergy, MatchMaker and DeepSynergy are shown in Fig. S3. Obviously, GNNSynergy performs better than the MatchMaker in most of cell lines. Besides, Fig. S4 shows the cell-line-specific MSE for GNNSynergy.

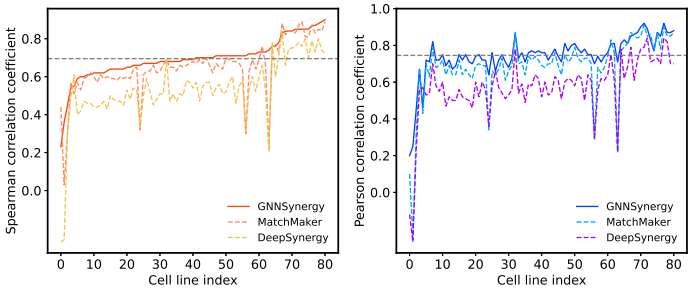

Figure S3: Spearman correlation coefficient and Pearson correlation coefficient comparison among GNNSynergy, DeepSynergy and MatchMaker. Here, MatchMaker is the best baseline as shown in our main manuscript. The gray horizontal dotted line represents the average score of GNNSynergy.

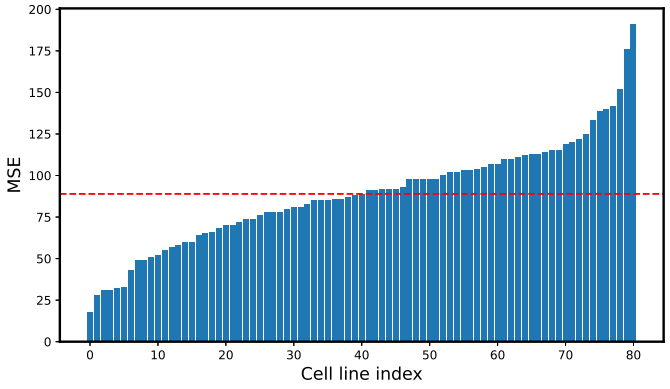

Figure S4: The MSE scores of GNNSynergy on each individual cell line. The red dotted line represents the average MSE score of GNNSynergy.

3.2 Attention Weights

As mentioned in the main manuscript, we adopted two weighting strategies to combine all sub-views, namely "Euqal Weights" and "Attention Weights". Here, we further explore the differences in the specific weights produced by these two strategies. Table S5 shows that the actual attention weights of 9 sub-views while the main-view cell is line SW-620.

Table S5: **The weights for different sub-view cell lines in large intestine, when the main view cell line is SW-620.**

Sub-view Cell Lines	Equal Weights	Attention Weights
sub-view 1 (HT29)	0.1111	0.1236
sub-view 2 (HCT116)	0.1111	0.1558
sub-view 3 (HCT-15)	0.1111	0.0953
sub-view 4 (KM12)	0.1111	0.1083
sub-view 5 (COLO 205)	0.1111	0.0417
sub-view 6 (HCC-2998)	0.1111	0.1699
sub-view 7 (LOVO)	0.1111	0.0519
sub-view 8 (SW837)	0.1111	0.0643
sub-view 9 (RKO)	0.1111	0.1893

3.3 Impact of DDS Graph Construction

Recall that we discussed the impact of using different combinations of graphs as input in the main manuscript. In addition, we further discussed the following situation. Unlike the 'One Graph' of the main manuscript, the variant 'Single Graph' here refers to using a single DDS graph to include all the drug combination pairs (i.e., we do not differentiate synergistic or antagonistic effects in this variant). The variant 'Two Graphs (t=0)' refers to using synergy graph and antagonism graph when threshold t is set as 0. The variant 'Two Graphs (t=10)' is the same as 'Two Graphs' in the main manuscript. As shown in Fig. S5, GNNSynergy with three DDS graphs achieves the best performance.

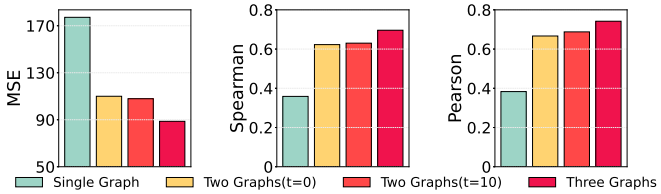

Figure S5: The performance comparison of three variants to construct the DDS graphs.

3.4 Case studies for novel drug combination prediction

As mentioned in our main manuscript, we found that 19 out of these 4,050 predicted drug pairs are considered as synergistic pairs in DrugCombDB. These 19 predicted pairs are listed in Table S6.

Table S6: **19 predicted drug combination pairs with literature support.**

#	Rank	Drug 1	Drug 2	Cell line
1	302	AURANOFIN	TRAMETINIB	NCI-H226
2	497	AURANOFIN	PD325901	NCI-H226
3	834	AURANOFIN	CISATRACURIUM BESYLATE	NCIH23
4	992	CISATRACURIUM BESYLATE	AURANOFIN	UWB1289
5	1207	AURANOFIN	CARFILZOMIB (PR-171)	SF-268
6	2192	AURANOFIN	TRAMETINIB	HOP-92
7	2356	CISATRACURIUM BESYLATE	AURANOFIN	LOVO
8	3219	CARFILZOMIB (PR-171)	AURANOFIN	LOVO
9	3454	ZALCITABINE	AURANOFIN	SR
10	3700	NILOTINIB	SORAFENIB	T98G
11	3704	NILOTINIB	VEMURAFENIB	T98G
12	3714	IMATINIB	NILOTINIB	T98G
13	3716	NILOTINIB	GEFITINIB	T98G
14	3722	SORAFENIB	VEMURAFENIB	T98G
15	3729	IMATINIB	SORAFENIB	T98G
16	3742	ERLOTINIB HYDROCHLORIDE	NILOTINIB	T98G
17	3907	ISONIAZID	BORTEZOMIB	HDLM-2
18	3909	LEFLUNOMIDE	BORTEZOMIB	HDLM-2
19	3925	PROCARBAZINE	BORTEZOMIB	HDLM-2